Annals of Diagnostic Pathology 46 (2020) 151523

Contents lists available at ScienceDirect

Annals of Diagnostic Pathology

journal homepage: www.elsevier.com/locate/anndiagpath

Original Contributions

mTOR pathway activation in focal cortical dysplasia

Kalpana Kumari[a], Mehar C. Sharma[a,*], Aanchal Kakkar[a], Prit B. Malgulwar[a], Pankaj Pathak[a], Vaishali Suri[a], Chitra Sarkar[a], Sarat P. Chandra[b], Mohammed Faruq[c]

[a] Department of Pathology, All India Institute of Medical Sciences, New Delhi, India
[b] Department of Neurosurgery, All India Institute of Medical Sciences, New Delhi, India
[c] Institute of Genomics and Integrative Biology - Council of Scientific and Industrial Research, New Delhi, India

ARTICLE INFO

Keywords:
Focal cortical dysplasia
Mammalian target of rapamycin
Epilepsy
TSC gene

ABSTRACT

Background: Focal cortical dysplasia (FCD) is a localized cortical malformation and considerable morphological overlap exists between FCD IIB and neurological lesions associated with Tuberous sclerosis complex (TSC). Abnormal mTOR pathway secondary to somatic mTOR mutation and TSC gene mutation linked to PI3K/AKT/mTOR pathway have supported the hypothesis of common pathogenesis involved. Role of converging pathway, viz. Wnt/β-Catenin and mTOR is unknown in FCD. We aimed to analyse FCD IIB for *TSC1/TSC2* mutations, immunoreactivity of hamartin, tuberin, mTOR and Wnt signalling cascades, and stem cell markers.

Materials and methods: Sixteen FCD IIB cases were retrieved along with 16 FCD IIA cases for comparison. Immunohistochemistry was performed for tuberin, hamartin, mTOR pathway markers, markers of stem cell phenotype, and Wnt pathway markers. Mutation analysis for TSC1 and TSC2 was performed by sequencing in 9 FCD cases.

Results: All FCD cases showed preserved hamartin and tuberin immunoreactivity. Aberrant immunoreactivity of phospho-P70S6 kinase, S6 ribosomal, phospho-S6 ribosomal and Stat3 was noted in FCD IIB, with variable phospho-4E-BP1 (45%) and absent phospho-Stat3 expression. Immunoreactivity for phospho-P70S6 kinase (100%), S6 ribosomal protein (100%) and Stat3 (100%) was noted in FCD IIA, but not for phospho-S6 ribosomal, phospho-4E-BP1 and phospho-Stat3. c-Myc immunoreactivity was noted in all FCD cases. Nestin (81%) and Sox 2 (88%) stained balloon cells in FCD IIB (44%), while in FCD IIA cases were negative. All FCD cases were immunopositive for Wnt, but were negative for β-Catenin and cyclin-D1. *TSC* mutations were detected in two cases of FCD IIB.

Conclusion: Abnormal mTOR pathway activation exists in FCD IIB and IIA, however, shows differential immunoreactivity profile, indicating varying degrees of dysregulation. Labelling of neuronal stem cell markers in balloon cells suggests they are phenotypically immature. *TSC1/2* mutation play role in the pathogenesis of FCD. Deep targeted sequencing is preferred diagnostic technique since conventional sanger sequencing often fails to detect low-allele frequency variants involved in mTOR/TSC pathway genes, commonly found in FCD.

1. Introduction

Malformations of cortical development (MCDs) include tuberous sclerosis complex (TSC), focal cortical dysplasia (FCD), and hemimegalencephaly (HMGE) [1]. These are the most common causes of multidrug-resistant epilepsy, and have been associated with aberrant mTOR signalling [2]. TSC is an autosomal dominant disorder resulting from mutations in *TSC1/TSC2* genes, which regulate the mTOR signalling cascade. While the primary molecular genetic defect and the link to mTOR pathway is well known in TSC, the role of *TSC1/2* alterations in the pathogenesis of FCD is not extensively studied [3]. Recently, a novel *TSC1* frameshift mutation has been described in a case of isolated FCD IIB [4]. The ILAE classification categorizes FCD into isolated Types I and II, based on architectural abnormalities in type I, presence of dysmorphic neurons and balloon cells in type IIA and IIB, respectively, while type III is associated with other epileptogenic lesions [5]. Considering the striking morphological similarities between FCD IIB and cortical tubers seen in TSC, it has been hypothesized that FCD is a "forme fruste" of TSC [6,7]. Ongoing studies have observed *TSC1* and *TSC2* sequence alterations, loss of heterozygosity and microsatellite instability and disease causing mutations in a series of FCD IIB and IIA patients [8-10]. Importantly, MCDs, including FCD, are

* Corresponding author at: Department of Pathology, All India Institute of Medical Sciences, New Delhi 110029, India.
E-mail address: sharmamehar@yahoo.co.in (M.C. Sharma).

https://doi.org/10.1016/j.anndiagpath.2020.151523

disorders involving the mTOR signalling pathway, however the cause is not well understood [11-13]. Subsequently, studies have also demonstrated somatic mTOR mutations in FCD involving PI3/AKT/mTOR pathway regulatory genes, based on detection of increased levels of phosphorylated ribosomal proteins [14-17]. In addition, somatic mutation of a tumor suppressor gene, PTEN, upstream of *TSC1/TSC2* gene has also been detected in FCD IIB [12]. Interestingly, a recent study highlighted that mild MCD/FCD I and FCD II/HMGE are two distinct genetic entities, while all FCD II/HMGE are mosaic mTORopathies [18]. Aberrant mTOR activation in balloon cells and dysmorphic neurons similar to that present in giant cells of tubers is previously well known [16,19,20]. However, the cellular origin and molecular phenotype of the heterogeneous cell population seen in FCD is still unknown [19,20]. It has also been hypothesized that these cytomegalic cells retain an immature stem-cell like phenotype, and the heterogeneous cell populations in FCD can be differentiated on the basis of their stem cell expression profile [19,21].

Balloon cells and cytomegalic neurons similar to that present in FCD IIB and tubers are seen in HMGE [18,22]. *TSC1/TSC2* complex promotes β-Catenin degradation and inhibits Wnt-mediated gene transcription. Aberrant expression and colocalization of Cyclin-D1 and Phospho-S6 ribosomal protein in cytomegalic cells in HMGE supports the role of two converging pathways, viz. Wnt/β-Catenin and mTOR linked to its neuropathology [22]. Mutations found in FCD IIB i.e. somatic gain-of-function variants in mTOR genes, as well as germline, somatic and two-hit loss-of-function variants in *TSC1/TSC2* has also been detected in HMGE patients using target gene sequencing [18]. Cotter et al., much earlier suggested that altered Wnt/Notch signalling pathway contributes in the pathogenesis of FCD and demonstrated altered cytoplasmic and reduced nuclear β-catenin immunostaining in the cytomegalic neurons [23]. While role of mTOR pathway is elucidated [22], the status of Wnt/β-Catenin pathway has not been adequately analyzed in FCD till date.

With this background, we aimed to detect alterations in *TSC1* and *TSC2* genes, to analyse the immunoexpression of their protein products tuberin and hamartin, to identify the presence of stem cell phenotype using stem cell markers, and to elucidate the role of stem cell markers, mTOR pathway and Wnt/β catenin pathway in the pathogenesis of FCD.

2. Materials and methods

Sixteen cases of FCD IIB and an equal number of FCD IIA resected for treatment of medically intractable epilepsy between 2008 and 2014 were retrieved from the archives of the Department of Pathology at our Institute. Clearance was obtained from the Institute Ethics Committee to conduct this study. Hematoxylin and eosin stained slides were reviewed independently for confirmation of diagnosis and classified as per ILAE 2011 classification by two neuropathologists (MCS, KK) [5]. Lesions showing presence of dysmorphic neurons, i.e. mal-oriented neurons with enlarged cell body and nucleus, were classified as FCD IIA. Those with balloon cells, i.e. cells with large cell body, eccentrically placed nucleus and opalescent glassy eosinophilic cytoplasm, were classified as FCD IIB. Clinical data was obtained.

2.1. Immunohistochemistry

Immunohistochemistry for the following monoclonal antibodies were performed in all cases with adequate tumor tissue: hamartin, tuberin; markers of mTOR pathway activation viz. phospho-p70S6 kinase (Thr389), S6 ribosomal protein, phospho-S6 ribosomal protein, phospho-4E-BP1 (Thr37/46), Stat3, phospho-Stat3; markers of Wnt pathway activation viz. Wnt, β-Catenin and cyclin D1, and markers of stem cell phenotype viz. c-Myc, nestin, Sox-2 and CD34. Universal labelled streptavidin biotin kit was used as the detection system (Dako, Glostrup, Denmark). Five micron thick sections cut from formalin-fixed paraffin-embedded (FFPE) tissue blocks were mounted on poly-L-lysine-coated slides. Sections were deparaffinized and rehydrated in descending grades of alcohol. Antigen retrieval was performed by boiling in citrate buffer (0.01 mol/L) at pH 6.0 in a microwave oven for 30 min. To diminish endogenous peroxide activity, slides were treated with 3% hydrogen peroxide in methanol for 30 min. After rinsing briefly with TRIS buffer, sections were overlaid with appropriately diluted primary antibody and incubated overnight at 4 °C in a humid chamber. Sections were washed in TRIS buffer, treated with the biotin-labelled secondary antibody for 60 min at room temperature, and then washed in TRIS buffer. Peroxidase-conjugated streptavidin was applied, and the sections were incubated at room temperature for 30 min. Sections were rinsed, stained with the chromogen diaminobenzidine for 5 to 10 min, washed, counterstained with hematoxylin, and then mounted. Sections from normal adult brain cortex from autopsies for deaths unrelated to central nervous system diseases were used as negative controls, while four specimens of SEGA known to be positive for these markers were taken as positive controls. Staining for phospho-p70S6 kinase, S6 ribosomal protein, phospho-S6 ribosomal protein, phospho-4E-BP1, Stat3 and phospho-Stat3 was estimated as follows: no staining: 0; faint positivity in < 10% of cells: 1+; moderate positivity in 10–50% of cells: 2+; strong positivity in ≥50% of cells: 3+. Only 2+ and 3+ staining was considered as positive [24].

2.2. DNA extraction and sequencing

DNA was extracted from all samples with adequate material in formalin-fixed paraffin-embedded (FFPE) tissue blocks. Eight serial sections of 10 μ thickness were cut from each block. RecoverAll™ Total Nucleic Acid Isolation Kit (Ambion, Texas, USA) was used to extract DNA as per the manufacturer's instructions. Exons 15 and 17 of *TSC1* gene, and exons 33, 39 and 40 of *TSC2* gene were selected for mutation analysis as they are most frequently mutated warm spots [25]. Polymerase chain reaction (PCR) was carried out using forward and reverse primers as described earlier [25], in a 10 μL reaction mixture containing 50 ng of DNA, 1 μL of 10× PCR buffer, 0.8 μL of 10 mM dNTPs, 0.25 μL each of forward and reverse primers, and 0.2 μL of AmpliTaq Gold PCR Master mix (Applied Biosystems, California, USA). Initial denaturation was carried out at 95 °C for 1 min, annealing at 57 °C for 45 s, and extension at 72 °C for 2 min. Bidirectional sequencing was performed using ABI 3730 sequencer (Applied Biosystems, California, USA). Mutation analysis was done using “Mutation Taster” online software, for predicting disease-causing potential of sequence alterations.

3. Results

3.1. Clinical features

Sixteen cases of FCD IIB and sixteen cases of FCD IIA were analyzed (Table 1). There was no significant difference between the mean age at onset of seizures in patients with FCD IIB (mean 4.5 years; range: birth to 10 years) and in those with FCD IIA (mean 5.6 years; range: birth to 15 years) ($p = 0.232$). However, those with FCD IIB underwent surgery at a significantly earlier age (mean: 9 years; range: 0.32 months to 28 years) as compared to those with FCD IIA (mean: 15 years; range: 0.5 to 51 years) ($p = 0.040$). Mean duration of seizures was 4.8 years (range: 0.32 months to 18 years) and 10 years (range: 0.5 to 36 years) in FCD IIB and FCD IIA, respectively ($p = 0.028$). Male predominance was noted in FCD IIA (M:F = 4.3:1) while FCD IIB occurred in both sexes nearly equally (1:1). FCD IIB cases were predominantly located in the frontal lobe (11/16 cases, 69%), while FCD IIA had a predilection for the temporal lobe (9/16 cases, 56%) ($p = 0.037$).

Table 1
Clinical details of FCD patients.

Case	Sex	Age at seizure onset (yrs)	Age at surgery (yrs)	Seizure duration (yrs)	FCD location on imaging	Histopathological diagnosis
1	M	1	2	1	LF	FCD II B
2	F	3	9	6	RF	FCD II B
3	M	6	12	6	RF	FCD II B
4	F	10	28	18	RF	FCD II B
5	M	6	10	4	RF	FCD II B
6	M	4	10	6	RF	FCD II B
7	M	9	27	18	RF	FCD II B
8	M	4	10	6	AO	FCD II B
9	F	3	4	1	RF	FCD II B
10	F	2.5	4	1.5	RT	FCD II B
11	F	2	4	2	RT	FCD II B
12	M	4	7	3	RF	FCD II B
13	F	1.5	3	1.5	Right hemisphere	FCD II B
14	M	At birth	0.32	0.32	LT	FCD II B
15	F	10	11	1	LF	FCD II B
16	F	1	2	1	LF	FCD II B
17	M	1	14	13	LT	FCD II A
18	M	8	24	16	MT	FCD II A
19	M	2	6	4	LF	FCD II A
20	M	At birth	0.5	0.5	LF	FCD II A
21	M	1	12	11	MT	FCD II A
22	M	13	20	7	RBF & RT	FCD IIA
23	F	5	16	11	RPO	FCD IIA
24	M	3	9	6	LF	FCD IIA
25	M	1	19	18	LT	FCD IIA
26	F	15	51	36	RT	FCD IIA
27	F	10	11	1	LF	FCD IIA
28	M	4	9	5	LT	FCD IIA
29	M	1	11	10	LT	FCD IIA
30	M	2	14	12	RT	FCD IIA
31	M	8	14	6	RF	FCD IIA
32	M	10	12	2	RF	FCD IIA

RF-Right frontal; LF-Left frontal; RT-Right temporal; LT-Left temporal; MT-Medial temporal; AO-Anterior opercular; LI-left insular; RBF; Left basifrontal; LBF-Left basifrontal; LO; Left occipital; RO; Right occipital; LTO; Left temporooccipital; RPO; Right parietooccipital.

3.2. Histopathological characteristics (Fig. 1a, b)

Microscopic examination revealed increased cortical thickening, cytoarchitectural disruption of cortical layering, and presence of dysmorphic neurons in FCD IIA. FCD IIB showed similar features along with presence of balloon cells lying singly and in clusters. In addition, grey and white matter junction was indistinct due to presence of numerous neurons interspersed between fibres of the white matter. Heterotopic neurons were encountered in the subcortical white matter and outside layer V.

3.3. Immunohistochemistry (Table 2)

3.3.1. Hamartin and tuberin

All cases of FCD IIB and IIA showed preserved immunoreactivity of hamartin and tuberin (Figs. 3a, b; 5a, b), similar to controls.

3.3.2. mTOR signalling cascade (Figs. 2a–f & 4a–f)

Strong immunostaining (3+) of phospho-P70S6 Kinase and S6 ribosomal protein was seen in balloon cells and dysmorphic neurons of all cases of FCD IIB. Diffuse strong (3+) immunostaining of phospho-S6 ribosomal and Stat3 was seen in 100% of FCD IIB cases in the balloon cells. Variable positivity for phospho-4E-BP1 was noted in seven cases of FCD IIB (3+ in 71%, 2+ in 29%) in the balloon cells. Robust immunostaining (3+) of phospho-P70 S6 Kinase, S6 ribosomal protein and Stat3 was noted in all FCD IIA cases in the dysmorphic neurons. However, phospho-S6 ribosomal and phospho-4E-BP1 were negative. None of the FCD IIA or IIB cases showed immunoreactivity of phosphorylated Stat3. Normal adult neocortex included as control showed faint immunostaining for phospho-p70S6 kinase, ribosomal S6, phospho-S6 ribosomal protein and Stat3 in the neurons while immunostaining for phospho-4E-BP1 and phospho-Stat3 were negative. Perilesional area showed similar staining pattern as normal brain cortex. Immunostaining for mTOR proteins (except for Phospho-Stat3) was seen in SEGA patients, used as control.

3.3.3. Stem cell markers (Figs. 3g–i & 5g–i)

Strong immunostaining of nestin (13/16, 81%) and Sox2 (14/16, 88%) was noted in the balloon cell population in FCD IIB cases, labelling both singly lying dispersed cells reaching up to the pial surface and cells deep in the white matter. All cases of FCD IIA were immunonegative for nestin and Sox2. CD34 immunostain showed bush-like staining pattern of balloon cells in 7 FCD IIB cases (44%). Interestingly, balloon cells located near the pial surface, deep white matter or at the grey-white matter junction showed CD34 staining which was confined to the cell membrane, but this was not observed in the neocortical parenchyma. Membranous (2 cases, 13%) or dendritic pattern (1 case, 6%) of CD 34 immunostaining was noted in 3 FCD IIA cases (19%). Dysmorphic neurons present in the neocortex showed membranous pattern while those in subcortical white matter or near to pial surface showed dendritic pattern of staining. Controls were negative for CD34.

3.3.4. Wnt/β-Catenin pathway (Figs. 3c–f & 5c–f)

Strong nuclear staining for c-Myc, and cytoplasmic as well as membranous immunostaining for Wnt was noted in dysmorphic neurons and balloon cells in all cases of FCD IIB and IIA. None of the cases showed nuclear staining for β-Catenin or cyclin D1. SEGA cases showed increased immunostaining for Wnt while normal cortex showed faint positivity in the neurons. c-Myc, β-catenin and cyclin D1 were negative in the controls.

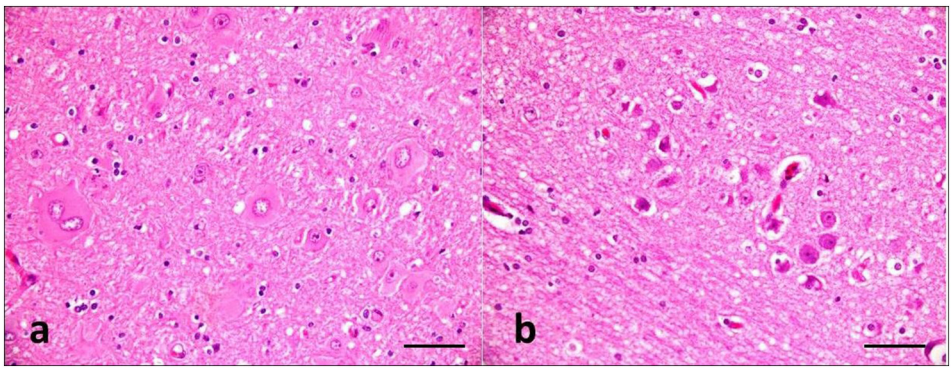

Fig. 1. Histomorphological features of focal cortical dysplasia: FCD IIB shows disruption of cortical layering, with balloon cells having large cell body and opalescent cytoplasm, and dysmorphic neurons in an indistinct neocortical layer (a). FCD IIA shows abnormal cortical layering with presence of maloriented dysmorphic neurons (b).

Table 2
Immunohistochemistry in cases of Focal cortical dysplasia.

	IHC marker	Company; dilution	FCD IIB (n = 16)			FCD IIA (n = 16)	
			IP (%)	Dysmorphic neurons	Balloon cells	IP (%)	Dysmorphic neurons
TSC proteins	Hamartin loss	Novacastra, UK; 1:400	0	−	−	0	−
	Tuberin loss	Acris, Germany; 1:25	0	−	−	0	−
mTOR pathway proteins	Phospho-P70 S6 Kinase (Thr389)	Cell Signalling, USA; 1;100	16 (100%)	+	+	16 (100%)	+
	S6 Ribosomal (5G10)	Cell Signalling, USA; 1:50	16 (100%)	+	+	16 (100%)	+
	Phospho-S6 Ribosomal (Ser235/236)	Cell Signalling, USA; 1:400	16 (100%)	−	+	0	−
	Phospho-4E-BP1 (Thr37/46)	Cell Signalling, USA; 1:1600	7 (44%)	−	+	0	−
	Stat3 (124 H6)	Cell Signalling, USA; 1:600	16 (100%)	−	+	16 (100%)	+
	Phospho-Stat3 (Tyr 705)	Cell Signalling, USA; 1:200	0	−	−	0	−
Stem cell markers	c-Myc	Santa Cruz, USA; 1:100	16 (100%)	+	+	16 (100%)	+
	Nestin	Abcam, USA; 1:200	13 (81%)	−	+	0	−
	Sox 2	Sigma, USA; 1:100	14 (88%)	−	+	0	−
	CD 34	Dako, Denmark; 1:50	7 (44%)	−	+	3 (19%)	+
Wnt/β catenin pathway	Wnt	Abcam, USA; 1:100	16 (100%)	−	+	16 (100%)	+
	β-Catenin	BD Transduction, USA;1:200	0	−	−	0	−
	Cyclin D1	Dako, Denmark; 1:100	0	−	−	0	−

FCD: focal cortical dysplasia; IP: immunopositivity.

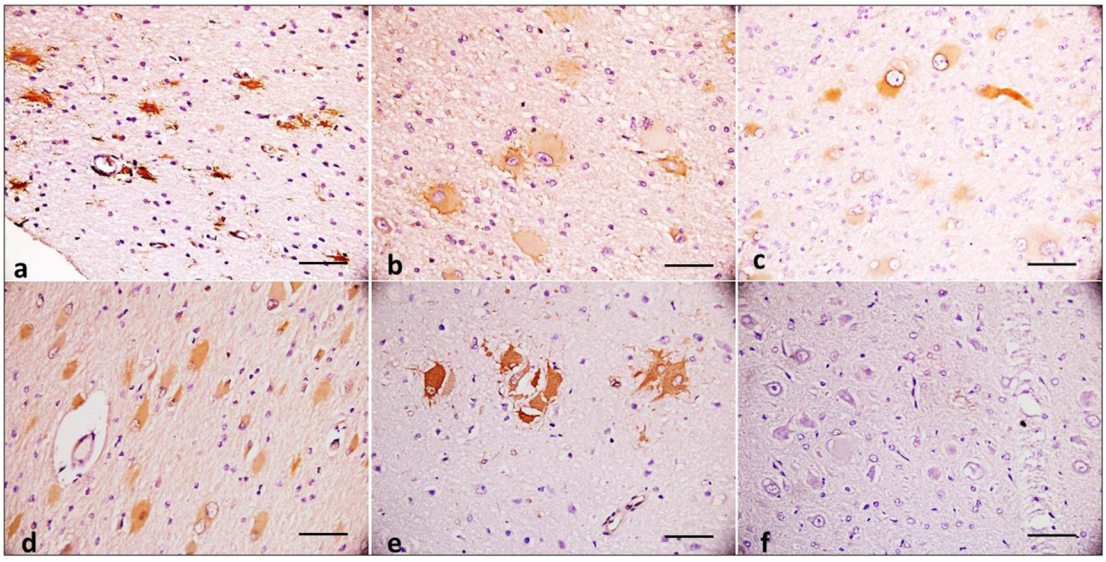

Fig. 2. FCD IIB showing strong nuclear immunoexpression for phospho-p70S6kinase (a). Strong cytoplasmic immunoexpression for S6 ribosomal (b). Strong nuclear immunoexpression for phospho-S6 ribosomal (c). Nuclear and cytoplasmic immunoexpression for phospho-4E-BP1 (d). Cytoplasmic immunoexpression for Stat3 while immunonegative for phospho-Stat 3 (e & f).

3.4. Mutation analysis

Mutation analysis was performed on nine cases (6 FCD IIB and 3 FCD IIA). Of these, two cases of FCD IIB showed pathogenic mutations in TSC1 (exon 15) and TSC2 (exon 33) genes, respectively (Table 3). Same mutation was detected in one of the SEGA patients [25]. In addition, polymorphisms were noted in TSC2 (exon 33) in three FCD IIB and two FCD IIA cases. On correlation with immunohistochemistry, cases showing mutation did not show loss of hamartin or tuberin. No difference was noted in clinical presentation of FCD IIB cases with and without mutation ($p = 0.5$).

4. Discussion

In recent years, mounting evidence has shown that not only TSC, but several distinct focal cortical malformations (FCMs) may be linked to aberrant activation of the mTOR pathway, constituting a spectrum of disorders known as “TORopathies” [2]. FCD can occur as an isolated lesion, or in association with tubers, or tumors like dysembryoplastic neuroepithelial tumor (DNET) and gangliogliomas [5]. Histological classification of FCD correlates with clinical and neuroimaging findings [5]. In the present study, the mean age at seizure onset, seizure duration and age at surgery for both groups were concordant with respect to results in the literature [26]. We also found that patients with FCD IIB presented with shorter duration of symptoms, greater frequency of seizure episodes and lower mean age at surgery, thus indicating severity of the seizure syndrome as compared to patients with FCD IIA who had significantly longer duration of seizures, and higher mean age at surgery. FCD IIB has mostly been reported to be extratemporal in location and tends to be multifocal, while FCD IIA is more prevalent in the temporal lobe, which is similar to our results [26,27].

We demonstrate activation of downstream effectors of mTOR signalling pathway, as evidenced by immunostaining for mTOR pathways markers viz. phospho-S6 ribosomal and phospho-4E-BP1 in FCD IIB. However, dysmorphic neurons in FCD IIA labelled only for phospho-P70 S6 Kinase and S6 ribosomal protein. Thus, the phosphorylation

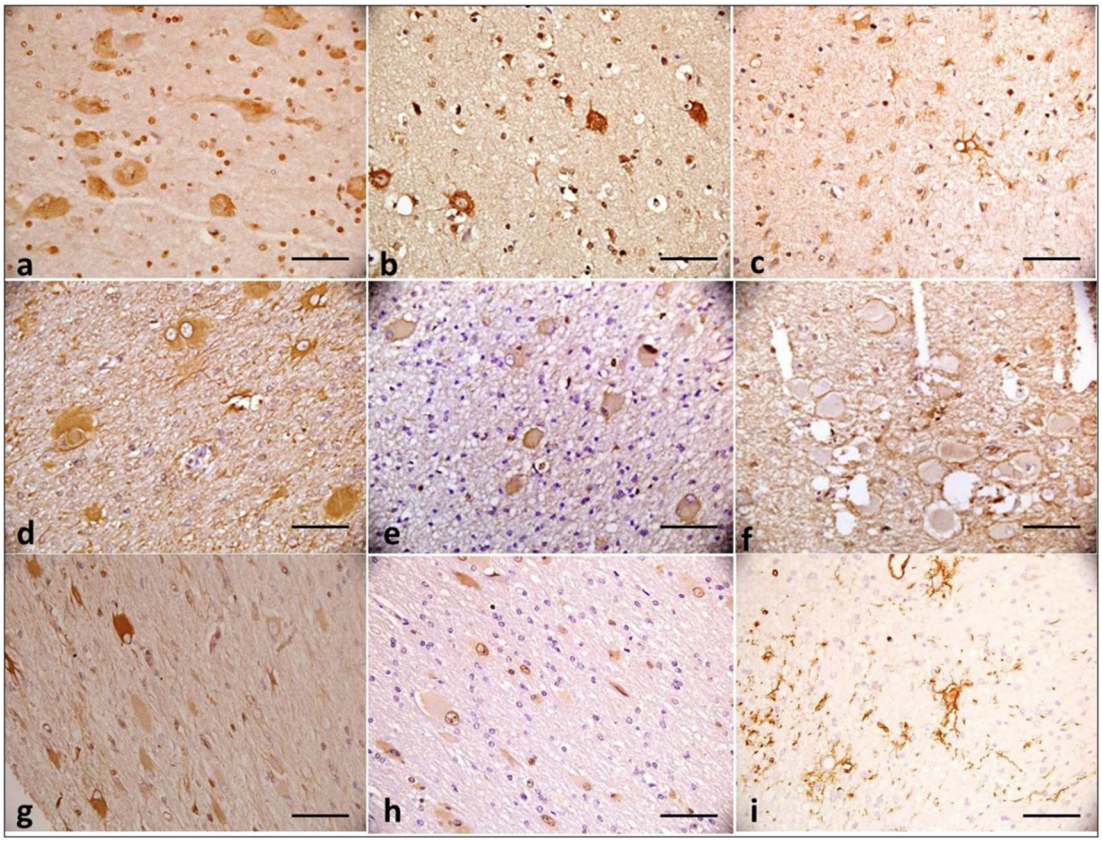

Fig. 3. FCD IIB showing retained immunoexpression of hamartin and tuberin in balloon cells and dysmorphic neurons (a & b). Membranous and cytoplasmic immunoreactivity for wnt in balloon cells (c). Increased cytoplasmic and nuclear expression for c-Myc in balloon cells and dysmorphic neurons (d). Negative immunostaining for cyclin D1 and β-Catenin (e & f). Strong cytoplasmic immunoexpression for nestin (g). Nuclear immunoexpression for Sox2 (h). Membranous dendritic and bush- like CD34 immunostaining of balloon cells present at grey white matter junction and lack of staining of same present in the neocortex (i).

profile of mTOR pathway components can distinguish FCD IIB from FCD IIA histomorphologically, though shares common clinical and pathogenic genetic variants [18]. Hence, partially differential immunostaining of mTOR pathway markers possibly suggests that FCD IIB and FCD IIA are a spectrum/gradient of the same disease process, with variable activation of different components of the mTOR pathway. Our results are also concordant with a previous study performed by Orlova et al. on 7 FCD IIB and 3 FCD IIA cases [21]. However, Lui et al. demonstrated prominent phospho-S6 labelling in dysmorphic neurons in FCD IIA in single case [28]. While most FCD patients respond to

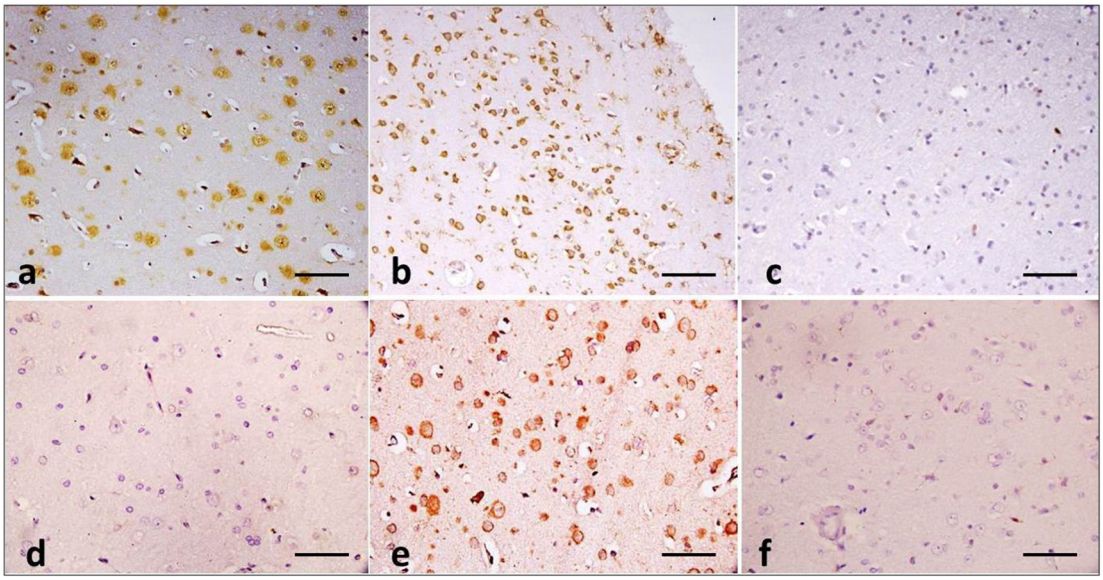

Fig. 4. FCD IIA showing nuclear immunoexpression for phospho-p70S6kinase (a). Strong cytoplasmic immunoexpression for S6 ribosomal (b). Negative immunostaining for phospho-S6 ribosomal and phospho-4E-BP1 (c & d). Cytoplasmic immunoreactivity for Stat3 while negative immunostaining for phospho-Stat3 (e & f).

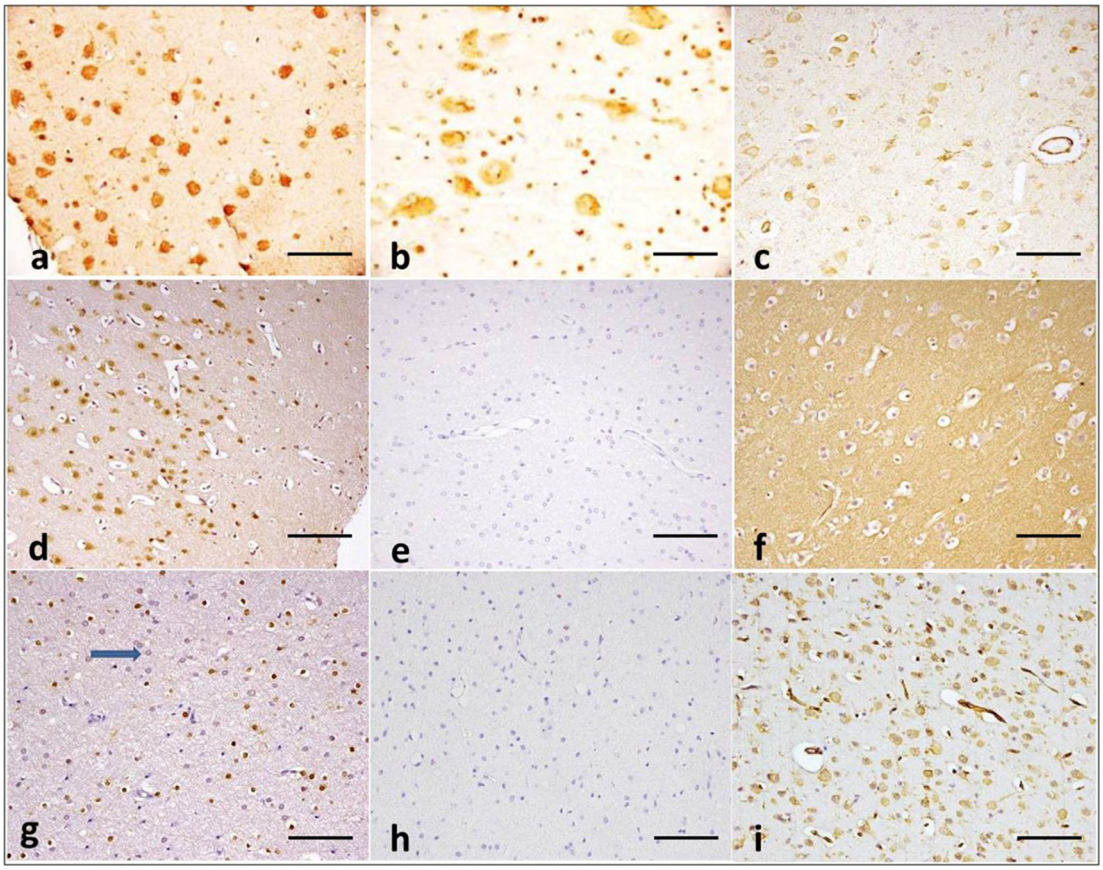

Fig. 5. FCD IIA showing retained immunoexpression of hamartin and tuberin in dysmorphic neurons (a & b). Membranous and cytoplasmic immunoreactivity for wnt (c). Increased cytoplasmic and nuclear expression for c-Myc (d). Negative immunostaining for cyclin D1, β-Catenin, nestin and Sox2 (e, f, g & h). Cytoplasmic CD34 immunostaining of dysmorphic neurons (i).

lesionectomy with seizure relief, a subset continue to have seizures in spite of normal MR imaging. In view of our results, it is likely that, based on histological type of FCD and evidence of activation of various components of the mTOR signalling cascade, those patients can be identified that may respond to mTOR inhibitors such as rapamycin which have already been proven efficacious in SEGA and other TSC-associated extracerebral lesions [29].

Heterogeneous cellular components of FCD have a striking histological resemblance to giant cells in SEGA and tubers from TSC patients [8]. Loss of function mutation in either *TSC1* and *TSC2* genes and known upstream inhibitors of mTOR leads to constitutive activation of mTOR cascade [11,13,14]. Hence, we attempted to elucidate the role of *TSC* gene alterations in the pathogenesis of FCD. Previous studies have shown LOH and MSI of *TSC1* gene within balloon cells in FCD IIB cases, suggesting a pathogenetic mechanism related to that of TSC [9,10]. Several allelic variants or polymorphisms at *TSC1* and *TSC2* loci have also reported in FCD IIB and FCD IIA [10,30]. We identified pathogenic mutations in two cases of FCD IIB. One of the mutations detected was similar to that present in a SEGA patient described in a previous study [25]. Of the two, one patient had similar history of seizures in an elder brother; however, neurocutaneous manifestations of TSC were absent. A novel *TSC1* frameshift mutation has recently been reported in 9-year-boy with family history of epilepsy and similar mutation occurring in index case mother, with absent TSC associated manifestations [4]. We also identified polymorphisms at *TSC2* locus in FCD IIA and FCD IIB cases, similar to previous studies [10,30]. Recent ongoing research confirms that FCD II harbours somatic/germline pathogenic variants with low-allele frequencies occurring in mTOR/TSC pathway genes [18]. Hence, it is critical to choose targeted deep sequencing as ideal diagnostic tool since conventional sanger sequencing fails to detect low-level mosaicism [18]. Similar to present study, strong phosphorylation of phospho-S6 ribosomal protein has been described in FCD II, irrespective of presence or absence of mTOR/TSC pathogenic variants; labelling them as mosaic mTORopathies [18]. We noted preserved

Table 3
Results of mutation analysis with corresponding hamartin and tuberin expression.

FCD cases (n = 9)	Gene/exon	Mutation	Immunohistochemistry	Polymorphism in TSC exon 33
Case 3 (FCD IIB)	TSC1 exon 15.1	Point mutation c.1792 A > T	Retained hamartin and tuberin expression	
Case 9 (FCD IIB)	TSC2 exon 33.2	Point mutation c.4364 G > A	Retained hamartin and tuberin expression	c.4276 C > G
Case 23(FCD IIA)			Retained hamartin and tuberin expression	c.4276 C > G
Case 20 (FCD IIB)			Retained hamartin and tuberin expression	c.4276 C > G
Case 12 (FCD IIB)			Retained hamartin and tuberin expression	c.4276 C > G
Case 22 (FCD IIA)			Retained hamartin and tuberin expression	c.4276 C > G

FCD: focal cortical dysplasia.

immunoexpression of hamartin and tuberin in FCD IIA and FCD IIB, which is in contrast to tubers in TSC. This may probably explain why they do not form mass lesions, as they may escape the "second hit", and are results of primary circuitry disturbances only [16]. It is possible that these mutations may produce an unstable or non-functional intact protein that is detectable by IHC.

Recent studies have demonstrated role of JAK/STAT3 signalling pathway in the induction of oncogene induced senescence (OIS), mediated by various cytokines [31]. An interesting feature of low grade gliomas is their propensity to spontaneously stop growing or even regress, which may be attributable to OIS [31,32]. A few studies have demonstrated that activation of mTOR pathway leads to dysregulated Stat3 expression in embryonic neural stem cells (eNSCs), and their premature differentiation into neuronal or astroglial lineage in subependymal nodules, SEGAs, and tubers [25,33]. We found increased cytoplasmic Stat3 immunostaining in balloon cells and dysmorphic neurons in FCD IIB and FCD IIA; however, showed negative immunostaining for phosphorylated Stat3. Hence, our findings suggest that, while hyperactivated mTOR pathway leads to dysregulated proliferation of cells, increased cytoplasmic Stat3 immunostaining in these cells imparts the ability to escape uncontrolled proliferation.

FCDs comprise a heterogeneous cell population, which shows differential expression of neurogenic stem cell markers [21,33]. Following mTORC1 activation there is enhanced translation of the transcriptional activator c-Myc [21,34], which regulates stem cell markers such as Sox2 [21]. Sox2 plays role in maintaining multi-potentiality of embryonic and mesenchymal stem cells and further regulates proliferation of nestin-positive neural progenitor cells through other intermediate stem cell markers [35,36]. Nestin, a class VI intermediate filament protein that is expressed in stem cells of the CNS, is virtually absent from nearly all mature CNS cells [36]. We demonstrate cytoplasmic immunostaining of nestin and nuclear staining of Sox2 in balloon cells in FCD IIB, throughout the thickness of the lesion, reaching up to the pial surface, and even in deep white matter, suggesting that balloon cells are phenotypically immature cells with altered migratory signals. In contrast to balloon cells in FCD IIB, dysmorphic neurons in FCD IIB and IIA showed negative nestin or Sox2 staining. This lack of stem cell marker expression probably reflects that the dysmorphic neurons are more differentiated, and have escaped some inhibitory pathway which leads to generation of balloon cells. Similar differences in the immunostaining of stem cell markers in dysmorphic neurons in FCD IIA compared to balloon cells in FCD IIB, have been demonstrated previously [21], thus delineating developmental lineage. Hence, we suggest that immunohistochemical staining pattern of these stem cell markers may serve as an adjunct to histopathology for differentiating FCD IIB from FCD IIA lesions.

CD34 is a cell adhesion and signal transduction molecule, whose aberrant immunoreactivity has been described in the dysplastic neurons of GGs [9]. We found cell membrane and dendritic staining pattern of CD34 in FCD IIB in balloon cells, which were located either within the white matter or at the grey-white matter boundary, but not in the neocortex. Our results are similar to a previous study which showed differential staining of CD34 in balloon cells present in the white matter, but not in those located in the neocortex [9]. This may suggest that CD34 immunoreactive balloon cells within the white matter are most undifferentiated with retained stemness, and are devoid of any migratory signals. This potential appears to decline in balloon cells located at neocortical sites which managed to reach the cortical plate, however, with dysregulated lamination.

Role of Wnt/β-Catenin pathway is not extensively studied in FCMs except for HMGE [22,37,38]. Cytoarchitectural disarray, characteristic balloon cells, association with intractable epilepsy and pathogenic mutation in *mTOR/TSC1/TSC2* gene are features common to both HMGE and FCD [18]. Hence, we aimed to elucidate the role of Wnt/β-Catenin pathway in FCD, and found overexpression of Wnt and c-Myc in FCD IIB and FCD IIA cases. Since Wnt is an embryonic protein which plays a pivotal role in establishment of cell size and cell cycle regulation, its overexpression may be responsible for cytomegaly in FCD [39]. However, as immunoreactivity for β-Catenin and cyclin D1 was not seen in our study, we suggest that β-Catenin-mediated gene transcription does not operate in FCD. In HMGE, there is increased immunoreactivity of cyclin D1 which results from enhanced β-Catenin mediated gene transcription [39]. Thus, increased immunostaining for c-Myc and Wnt suggests that they may be responsible for the formation of cytomegalic cells; however, this process appears to be independent of β-catenin and cyclin D1, significantly pointing towards a hamartomatous histogenesis rather than a neoplastic one.

5. Conclusion

Abnormal mTOR pathway activation exists in FCD IIB and FCD IIA; however, there is a differential protein immunostaining profile between these groups. Expression of neuronal stem cell markers in balloon cells suggests that these cells are phenotypically immature and distinct from dysmorphic neurons in FCD IIA. *TSC1/2* mutations play role in the pathogenesis of FCD. Deep targeted sequencing is preferred diagnostic technique since conventional sanger sequencing often fails to detect low-allele frequency variants in mTOR/TSC pathway genes, commonly found in FCD.

Compliance with ethical standards

All authors declare no potential conflicts of interest (financial or non-financial). Informed consent was obtained from the patient. No animals were involved in the study.

References

[1] Barkovich AJ, Guerrini R, Kuzniecky RI, Jackson GD, Dobyns WB. A developmental and genetic classification for malformations of cortical development: update 2012. Brain 2012;135:1348–69.
[2] Crino PB. Focal brain malformations: a spectrum of disorders along the mTOR cascade. Novartis Found Symp 2007;288:260–70.
[3] Crino PB, Nathanson KL, Henske EP. The tuberous sclerosis complex. N Engl J Med 2006;355:1345–56.
[4] Hoelz H, Coppenrath E, Hoertnagel K, et al. Childhood onset epileptic encephalopathy associated with isolated focal cortical dysplasia. Clin EEG Neurosci 2017:1–5.
[5] Blumcke I, Thom M, Aronica E, et al. The clinicopathologic spectrum of focal cortical dysplasias: a consensus classification proposed by an adhoc task force of the ILAE Diagnostic Methods Commission. Epilepsia 2011;25:158–74.
[6] Barkovich AJ, Kuzniecky RI, Jackson GD, Guerrini R, Dobyns WB. A developmental and genetic classification for malformations of cortical development. Neurology 2005;65:1873–87.
[7] Holmes GL, Stafstrom CE. The Tuberous Sclerosis Study Group. Tuberous sclerosis complex and epilepsy: recent developments and future challenges. Epilepsia 2007;48:617–30.
[8] Becker AJ, Urbach H, Scheffler BJ, et al. Focal cortical dysplasia of Taylor's balloon cell type: mutational analysis of the TSC1 gene indicates a pathogenic relationship to tuberous sclerosis. Ann Neurol 2002;52:29–37.
[9] Fauser S, Becker A, Schulze-Bonhage A, et al. CD34-immunoreactive balloon cells in cortical malformations. Acta Neuropathol 2004;108:272–8.
[10] Majores M, Blumcke I, Urbach H, et al. Distinct allelic variants of TSC1 and TSC2 in epilepsy-associated cortical malformations without balloon cells. J Neuropathol Exp Neurol 2006;64:629–37.
[11] Ljungberg MC, Bhattacharjee MB, Lu Y, et al. Activation of mammalian target of rapamycin in cytomegalic neurons of human cortical dysplasia. Ann Neurol 2006;60:420–9.
[12] Schick V, Majores M, Engels G, et al. Activation of Akt independent of PTEN and CTMP tumor-suppressor gene mutations in epilepsy-associated Taylor-type focal cortical dysplasias. Acta Neuropathol (Berl) 2006;112:715–25.
[13] Schick V, Majores M, Engels G, et al. Differential PI3K-pathway activation in cortical tubers and focal cortical dysplasias with balloon cells. Brain Pathol 2007;17:165–73.
[14] Miyata H, Chiang ACY, Vinters HV. Insulin signaling pathways in cortical dysplasia and TSC-tubers: tissue microarray analysis. Ann Neurol 2004;56:510–9.
[15] Jansen LA, Mirzaa GM, Ishak GE, et al. PI3K/AKT pathway mutations cause a spectrum of brain malformations from megalencephaly to focal cortical dysplasia. Brain 2015;138:1613–28.
[16] Lin YX, Lin K, Liu XX, et al. PI3/AKT pathway polymerase chain reaction (PCR) array analysis in epilepsy induced by type II focal cortical dysplasia. Genet Mol Res 2015;14(3):9994–10000.
[17] Moller RS, Sarah W, Chipaux M, et al. Germline and somatic mutations in the MTOR

gene in focal cortical dysplasia and epilepsy. Neurol Genet 2016;2:118.
[18] Baldassari S, Ribierre T, Marsan E, Adle-Biassettes H, et al. Dissecting the genetic basis of focal cortical dysplasia: a large cohort study. Acta Neuropathol 2019;138:885–900.
[19] Baybis M, Yu J, Lee A, et al. mTOR cascade activation distinguishes tubers from focal cortical dysplasia. Ann Neurol 2004;56(4).
[20] Rossini L, Medici V, Tassi L, et al. Layer specific gene expression in epileptogenic type II focal cortical dysplasia. Normal looking neurons reveal the presence of hidden laminar organization. Acta Neuropathol Commun 2014;2:45.
[21] Orlova KA, Tsai V, Baybis M, et al. Early progenitor cell marker expression distinguishes type II from type I focal cortical dysplasia. J Neuropathol Exp Neurol 2010;69:850–63.
[22] Aronica E, Boer K, Baybis M, Yu J, Crino P. Co-expression of cyclin D1 and phosphorylated ribosomal S6 proteins in hemimegalencephaly. Acta Neuropathol 2007;114:287–93.
[23] Cotter D, Honavar M, Lovestone S, et al. Disturbance of Notch-1 and Wnt signalling proteins in neuroglial balloon cells and abnormal large neurons in focal cortical dysplasia in human cortex. Acta Neuropathol 1999;98:465–72.
[24] Chan JA, Zhang H, Roberts PS, et al. Pathogenesis of tuberous sclerosis subependymal giant cell astrocytomas: biallelic inactivation of TSC1 or TSC2 leads to mTOR activation. J Neuropathol Exp Neurol 2004;63:1236–42.
[25] Kumari K, Sharma MC, Kakkar A, et al. Role of mTOR signaling pathway in the pathogenesis of subependymal giant cell astrocytoma – a study of 28 cases. Neurol India 2016;64:988–94.
[26] Fauser S, Huppertz HJ, Bast T. Clinical characteristics in focal cortical dysplasia: a retrospective evaluation in a series of 120 patients. Brain 2006;29:1907–16.
[27] Fauser S, Essang C, Alltenmuller DM, Staack AM, Steinhoff BJ, Strobl K. Long-term seizure outcome in 211 patients with focal cortical dysplasia. Epilepsia 2015;56:66–76.
[28] Liu J, Reeves C, Michalak Z, et al. Evidence for mTOR pathway activation in a spectrum of epilepsy-associated pathologies. Acta Neuropathol Commun 2014;2:71.
[29] Wong M. A critical review of mTOR inhibitors and epilepsy: from basic science to clinical trials. Expert Rev Neurother 2013(6):657–69.
[30] Schonberger A, Niehusmann P, Urbach H, et al. Increased frequency of distinct TSC2 allelic variants in focal cortical dysplasia with balloon cells and mineralization. Neuropathol 2009;29:559–65.
[31] Kojima H, Inoue T, Kunimoto H, Nakajima K. IL-6-STAT signalling and premature senescence. JACKSTAT 2013;2:e25763–6.
[32] Magri L, Cambiaghi M, Cominelli M, et al. Sustained activation of mTOR pathway in embryonic stem cells leads to development of tuberous sclerosis complex-associated lesions. Cell Stem Cell 2011;9:447–62.
[33] Lamparello P, Baybis M, Pollard J, et al. Developmental lineage of cell types in cortical dysplasia with balloon cells. Brain 2007;130:2267–76.
[34] Fults D, Pedone C, Dai C, Holland EC. MYC expression promotes the proliferation of neural progenitor cells in culture and in vivo. Neoplasia 2002;4:32–9.
[35] Alonso MM, Diez-Valle R, Manterola L, et al. Genetic and epigenetic modifications of Sox2 contribute to the invasive phenotype of malignant gliomas. PLoS One 2011;6:e26740.
[36] Jin Z, Liu L, Bian W, Chen Y, Xu G, Cheng L. Different transcription factors regulate nestin gene expression during P19 cell neural differentiation and central nervous system development. J Biol Chem 2009;284:8160–73.
[37] Yu H, Pardoll D, Jove R. STATs in cancer inflammation and immunity. A leading role for STAT3. Nat Rev Cancer 2009;9:798–809.
[38] Crino PB. Molecular pathogenesis of focal cortical dysplasia and hemimegalencephaly. J Child Neurol 2004;19:330.
[39] Mak BC, Takemaru K, Kenerson HL, Moon RT, Yeung RS. The tuberin-hamartin complex negatively regulates β-catenin signaling activity. J Biol Chem 2003;278:5947–51.